EUROPEAN JOURNAL OF MATERIALS SCIENCE AND ENGINEERING
Volume 8, Issue 3, 2023: 128-141 | www.ejmse.ro | ISSN: 2537-4338

EJMSE

DOI: 10.36868/ejmse.2023.08.03.128

INVESTIGATIONS RELATED TO THE OPPORTUNITY OF USING FURNACE SLAG IN THE COMPOSITION OF ROAD CEMENT CONCRETE

Liliana Maria NICULA[1,2*], Daniela Lucia MANEA[1], Dorina SIMEDRU[3], Mihai Liviu DRAGOMIR[1*]

[1]Faculty of Civil Engineering, Technical University of Cluj-Napoca,
15, Daicoviciu Street, 400114 Cluj-Napoca, Romania
[2]University of Oradea, Faculty of Construction, Cadastre and Architecture, 4,
B.S. Delavrancea Street, 410058, Oradea, BH, Cluj-Napoca, Romania
[3]Research Institute for Analytical Instrumentation Subsidiary, National Institute for Research and Development for Optoelectronics INOE 2000, 67 Donath Street, 400293 Cluj-Napoca, Romania

Abstract

BFS blast furnace slag presentation of the challenges and opportunities is related to the use as a substitute of Portland cement, respectively of natural sand in the composition of road cement concretes. The inclusion of BFS in the composition of road concrete is an ecological approach from the point of view of reducing the consumption of non-renewable materials. A rational design of road concrete composition requires knowledge of the physical-mechanical properties of BSF with favorable and unfavorable impact on the durability of road concrete. Aspects of the impact of the quality of GGBS granulated and ground blast furnace slag as well as the properties of ACBFS air-cooled blast furnace slag crushed aggregates were analyzed in this article. Although all the physical-mechanical properties books are suitable for the slag powders inclusion in the road concretes composition, the high content of CaO-free and C_3A limits the substitution of cement with GGBS to prevent the occurrence of degradation during the exploitation period. ACBFS aggregates have been proven to be non-reactive to alkalis in cement, thus being suitable for inclusion in road cement concrete compositions. The increased values of the water absorption coefficient, respectively of the fineness modulus of the ACBFS type aggregates compared to natural sand, the reduction of the workability of the road concrete and the increase of the water/binder ratio. Finally, for the design of road concrete compositions with slag, preliminary tests were carried out on three series of mixtures, in which Portland cement was replaced by 15% GGBS and natural sand by 25% and 50% ACBFS respectively. The optimal slag road concrete recipe was established based in: increased workability (an important characteristic of road concretes), a low water/binder ratio and a 7-day compressive strength close to the control sample.

Keywords*: road concrete with slag, the oxide composition, activity index, mortar microstructure, water absorption coefficient, workability, compression strength.*

Introduction

Concrete is the most commonly used building material, the construction industry worldwide records an annual production of 1.53 tons [1]. Ordinary concrete contains about 12% cement and 80% aggregate by total weight.

The 1.6 billion tons of cement produced worldwide corresponds to a carbon footprint of 7% of the total carbon footprint in the atmosphere [2]. Current research highlights a number of industrial wastes that can be used as binders in cement-based mixes with the aim of minimizing

*Corresponding author: liliana.nicula@infra.utcluj.ro

the carbon footprint as well as neutralizing quantitatively important industrial wastes [3–11]. However, a sustainable solution for ecological production of pavement concrete would be to use industrial by-products such as blast furnace slag, steel slag, copper slag, granite dust aggregates and natural dolomite aggregates as alternative aggregates [12–15].

In this context, BSF blast furnace slag resulting as a by-product from the steel industry represents a sustainable source for the substitution of conventional materials in the composition of concrete. Globally, China is the largest producer and consumer of steel with a production of about 10^9 tons, a volume that accounts for over 50% of global steel production. We know from the literature [16] that every ton of crude steel produces 0.3 tons of BSF slag.

In our country, the Galati Iron and Steel Plant reported production of 2.35 million tons of steel in 2021, resulting in 700,000 tons of blast furnace slag [17].

In the solid state, BSF slag can have a crystalline or amorphous-glassy structure. The crystallinity of the slag mainly depends on the way the melt is cooled. When molten slag is rapidly cooled by water, it tends to have a disordered (amorphous) structure that gives it certain cementitious properties after grinding. However, slow cooling in air results in the molten slag having relatively good crystallinity with little or no reactivity [18].

Most of the research studies the use of GGBS as a substitute for cement in concrete production [19–21].

Granulated blast furnace slag and air-cooled blast furnace slag have been used to replace both fine and coarse aggregates in the concrete composition [18], [22–24]. The use of GGBS and ACBFS in Portland cement-based materials has a replacement rate limitation as too high a level can have adverse effects on the performance of cement-based materials [25], [26].

Based on the study carried out on cement mortars with different percentages of substitution of the usual materials by blast furnace slag [27], this paper presents the experimental results obtained by using blast furnace slag in the composition of road concrete, in percentages of 15% GGBS of the cement mass or 25% and 50% ACBFS of the natural sand mass.

The chemical and physical-mechanical properties of granulated and non-granulated blast furnace slag, as well as the influence of chemical components on the properties of hardened and fresh concrete are examined. At the same time, the evolution of the microstructure of the mortar under the influence of 50% GGBS and the standard mortar was studied by SEM technology (Scanning Electron Microscope) and EDX (Energy Dispersive X-ray Analysis), followed by the evaluation of the activity index at the age of 7 days based on the mechanical resistance ratio between the mortar with 50% GGBS and the standard mortar.

Materials and Methods

Materials

Portland cement, CEM I 42.5R was supplied by Romcim, CRH Company, with a specific surface area of 331 m^2/kg and technical properties according to EN 197-1. The granulated blast furnace slag GGBS, was supplied by Plant Steel of Galati and ball milled to a specific surface area of 330 m^2/kg (63 m), the same as that of Portland cement. ACBFS (0/8) mm air-cooled blast furnace slag aggregate was obtained from Galati Steel Works and later ground to fine (0/4) mm aggregate using the UTCN laboratory bead mill. The quality assurance of natural sand (0/4) mm and gravel (4/8) mm was controlled according to EN 12620. For the screening of quarry-crushed (16/25) mm, the geometric and physical-mechanical properties correspond to the requirements of SR 667 [28], or EN 13043 for the grade (8/16) mm. The granulation of the total mixture of aggregates used is within the limit values specified by NE 014 [29] and is shown in Table 1.

Table 1. Graininess of the aggregates for the total mixture, minimum and maximum limit according to NE 014.

Sieve (mm)	0.125	0.25	0.5	1	2	4	8	16	25
				sieve passing (%)					
S0/0	2.70	5.01	15.10	25.27	32.91	45.39	62.53	82.12	100
S15/25	3.30	5.75	14.79	24.22	32.14	45.39	62.53	82.12	100
S15/50	3.90	6.50	14.83	23.17	31.37	45.39	62.53	82.12	100
Min.	1.44	2.38	4.25	8.00	14.00	23.75	38.11	63.00	95.00
Max.	6.22	9.19	15.13	27.00	34.50	46.50	62.55	83.00	100.00

Methods

Proportional oxide components were analyzed for the GGBS slag, the degree of saturation in the lime S_k was calculated using the Kuhl formula (eq.1) as in work [30], and the content of tricalcium aluminate C_3A was calculated using the Bogue formula (eq.2), and the activity index of the slag powders after 7 days calculated with (eq.3).

$$S_k=\frac{\%CaO}{2.8\%\ SiO_2+1.1\%Al_2\ O_3+0.7\%Fe_2O_3}\ , \tag{1}$$

$$C_3A=2.65Al_2O_3-1.69Fe_2\ O_3\ , \tag{2}$$

$$IA_7=\frac{fc_{GGBS}}{fc_{cement}}x100\ , \tag{3}$$

In the above relationship, (fc_{GGBS}) represents the average compressive strength (MPa) of the mortar made with 50:50 slag and cement and (fc_C) is the average compressive strength (MPa) of the reference mortar made from Portland cement according to EN 15167-1.

SEM-EDX electron microscopy and energy dispersive X-ray analyzes were performed on the mortar made with 50% GGBS and on the standard 100% Portland cement mortar aged 7 days. SEM-EDX measurements were performed at room temperature using a scanning electron microscope (VEGAS 3 SBU, Tescan, Brno-Kohoutovice, Czech Republic) with a Quantax EDX XFlash (Bruker, Karlsruhe, Germany) detector. Samples of ~4 mm^2 were attached to a SEM stub with carbon tape.

For the ACBFS aggregates, the fineness mode calculated as the sum of the total fractions retained on the site series was determined according to EN 12620, the water absorption coefficient WA_{24} according to EN 1097-6 and the alkali-silica reaction using the chemical method according to SR 5440 [31]. The assessment of the potential reactivity of the aggregates containing low crystallizing forms of silica (SiO_2) with the alkalis in the cement was calculated using (eq.4).

$$S_c=\frac{(A_1-A_2\ )x1000x1000}{5x60.06}, \tag{4}$$

where:

Sc is the concentration of dissolved silicon dioxide, in mmol/dm^3.

A_1 the amount of silicon dioxide in g found in 100 cm3 of dilute solution.

A_2 the amount of silicon dioxide, in g, found in 100 cm3 of the diluted blank solution.

60.06 is the molecular mass of silicon dioxide, in g.

The preliminary tests were carried out on three series of road concrete with different recipes, on which tests were carried out on fresh concrete according to EN 12350-6 for bulk density, EN 12350-4 for the degree of compaction and EN 12350-7 for trapped air. The 7-day compressive strength was determined on hardened concrete according to EN 12390-3.

For each mix, three 150 mm side cube-shaped samples were prepared and the quantities are summarized in Table 2 with the following abbreviations: C-cement, GGBS granulated and ground blast furnace slag (replacement for cement), NA- natural sand, ACBFS – air-cooled blast

furnace slag (replacement for natural sand), CA 4/25 – coarse aggregates (4/25) mm, SP – superplasticizer additive, AA – air entraining additive and images in Fig. 1. The design parameters of the recipes are summarized in Table 3.

a) b) c)

Fig. 1. Photo images taken during the preparation of concretes: a) Entrapped air measurement; b) Specimens in fresh and hardened state; c) Compressive strength test

Table 2. The quantities of materials per m^3.

Mix Kg/m^3	S0/0-I	S15/25-I	S15/50-I	S0/0-II	S15/25-II	S15/50-II	S0/0-III	S15/25-III	S15/50-III
C	390	331.50	331.50	370	314.50	314.50	370	314.50	314.50
GGBS	-	58.50	58.50	-	55.50	55.50	-	55.50	55.50
Binder (l)	390	390	390	370	370	370	370	370	370
Water (w)	159.93	161.40	162.75	150.40	159.93	163.40	151.68	154.51	155.85
w/l	0.410	0.414	0.417	0.406	0.432	0.442	0.41	0.418	0.421
NA_0/4	600.05	450.04	300.02	618.87	464.15	309.42	654.70	490.33	326.44
ACBFS	-	150.01	300.03	-	154.72	309.42	-	163.44	326.15
CA_4/25	1275	1275	1275	1256.48	1257.17	1256.42	1215.88	1214.16	1212.48
Totally aggregated	1875	1875	1875	1875	1875	1875	1871	1868	1865
SP	6.98	7.71	8.89	5.57	5.71	5.92	5.55	6.18	6.29
AA	1.95	1.95	1.95	0.74	0.74	0.74	0.74	0.74	0.74

Table 3. Design parameters of road concrete composites in accordance with NE 014 and EN 206.

Cement dosage (kg/m^3)	(w/l)	Compaction degree (%)	Air occluded (%)	The density appearance (kg/m^3)	fcm 28 days (MPa)	fcf,fl 28 days (MPa)
min. 360	max. 0.45	1.15÷1.35	5÷6	2390 ±30 (sliding formwork) 2400 ±40 (fixed formwork)	min. 50	min.5.5

Results and discussions

` Characterization of the physico-mechanical properties of GGBS slag

The oxide composition and properties of the granulated slag in Tables 4 and 5 have been given up to the limits of SR 648 [32] and EN 15167-1. The influence of the content of free CaO, tricalcium aluminate C_3A and the activity index IA was analyzed after 7 days, determined on standard cement mortar and on mortar with 50% GGBS.

Table 4. Oxide composition of GGBS blast furnace slag (%).

SiO_2	CaO	Al_2O_3	MgO	FeO	MnO	K_2O	Na_2O	S
38.10	40.80	9.50	8.10	0.56	0.23	0.68	0.30	0.69

Note: (*) Chemical characteristics tested by the manufacturer

Table 5. Physico-mechanical characteristics of GGBS slag powder.

Physical-mechanical characteristics	Recorded values	Limits EN 15167-1 and SR 648
* Stability (Le Chatelier), (mm)	0	-
* Chloride, (%)	0.002	≤ 0,10
* Humidity (%)	6.73	-
* Vitreous mass content (%)	95	-
* Magnesium oxide MgO, (%)	8.10	≤ 18
The amount (CaO+MgO+SiO2)	87	≥ 2/3
The report (CaO+MgO)/SiO_2	1.28	≥ 1.0
The report (CaO/SiO_2)	1.07	1.1...1.4
The content of free calcium oxide CaO, (%)	8.92%	Max 2%
The content of tricalcium aluminate C_3A, (%)	24.23%	6…12
Compressive strength fc-7days for standard mortar (MPa)	34.40	
Compressive strength fc-7days for mortar with 50% GGBS (MPa)	20.34	
Activity index at 7 days (%)	59	Min 45

Note: (*) Physio-mechanical characteristics tested by the manufacturer

The analyzed slag has favorable properties in terms of stability, content of chlorides, magnesium oxide and glassy mass, but has a high-water absorption capacity (6.73% moisture), which reduces the workability of the concrete. The superunit ratio between the sum of calcium and magnesium oxides and the sum of silicon and aluminum oxides in Table 4, matches the slag used as the basis [33] and the ratio of 1.07 (superunit) between calcium oxide and silicon indicates a effective hydraulic activity [4], [34]. The correlation between the two characteristics shows that the more basic the slag, the higher the hydraulic activity of the slag in the presence of alkaline activators [4]. The 97.06% concentration of silicon, calcium, aluminum, magnesium and iron oxides accumulated in the GGBS slag exceeds the 70% limit set for pozzolanic materials according to the D 6868 standard [4], [35]. The sum of calcium, magnesium and silicon oxide is 87% and the ratio of 1.28 between the sum of calcium and magnesium oxide to silicon oxide is above the limit according to SR EN 15167-1. The degree of saturation in the lime (Sk) of 31.88% (calculated with Equation 1), which is required to saturate the acidic oxides (SiO_2, Al_2O_3 and Fe_2O_3), shows a proportion of 8.92% of unbound calcium oxide (CaO-free) by burning process of ores. Because CaO-free hydrates slowly over time, it creates expansion in the concrete. For cement, the expansion has no significant effects if the proportion of free CaO is less than 2% of the cement clinker mass [36]. This limit is respected if the replacement of cement by GGBS in cementitious concrete compositions is below 22%. To prevent sulphate corrosion of concrete, the content of tricalcium aluminate C_3A is limited to a maximum of 12%. Application of Bogue (eq.2) results in a grade of 24.23% tricalcium aluminate, which limits the substitution of GGBS for cement to less than 50% grade. The IA activity index for GGBS slag determined at 7 days recorded a value of 59% above the 45% limit specified in Table 5.

Scanning Electron Microscopy, SEM, was used to study the surface morphology of the early 100% cement 50% GGBS mortar. The images obtained are shown in Fig. 2 and Table 6.

At lower magnitude the MI surface (Fig. 2a) with Mag.259.64x, showed a compact surface with large air holes (r = 61.14 μm) spaced >600 μm. The MII surface (Fig. 2c) with Mag.302.91x, showed a porous surface with smaller air holes (r in the range from 8.52 to 20.12 μm) at smaller intervals (from 59.29 to 452.76 μm) and large cracks. At a higher magnitude, the MI surface (Fig. 2b), with Mag. 1.3kx, still shows a compact surface with few small pores (r varies from 1.92 to 2.21 m) and small cracks. MII surface (Fig. 2d), with Mag 747.96x, pores with a radius of 3.58–7.07 m and a large number of smaller cracks are identified, indicating a more porous surface [37], [38] It is believed that the difference in surface morphology of MI compared to MII is due to slag having slower hydration reaction and slower heat release than Portland cement [39].

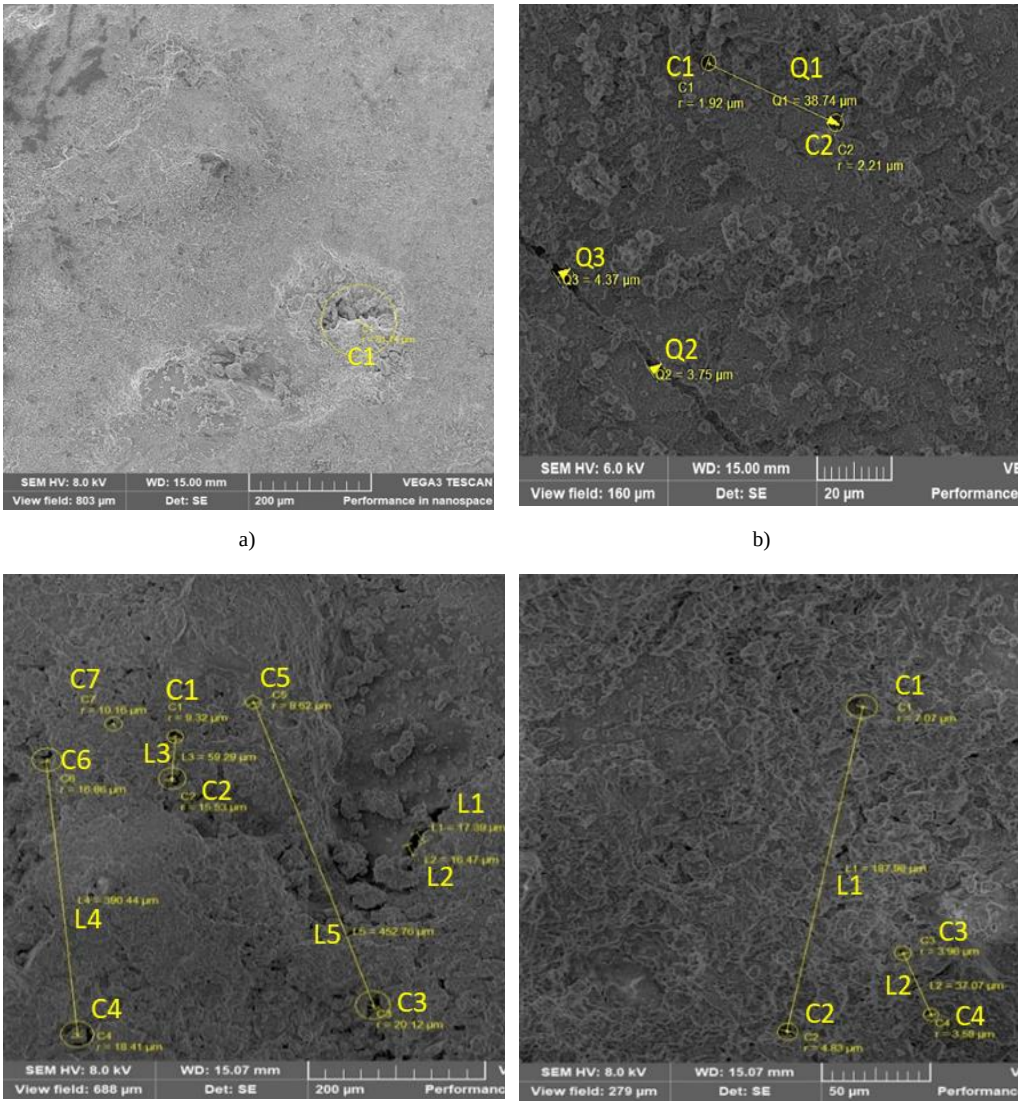

Fig. 2. Pore structure of: a), b) MI-100% cement; c), d) MII -50% GGBS mortar samples

Table 6. Pore radius and pore distance measured in mortar sample M I-100% cement and M II-50% GGBS.

Sample	Pore identification code	Pore radius (µm)	Distance identification code (Ci-Ci+n)	Distance (µm)
M I	C1	61.14	-	-
M I	C1	1.92		
	C2	2.21	Q1(C1-C2)	38.78
			Q2	3.75
			Q3	4.37
M II			L1	17.39
	C1	9.32	L2	16.47
	C2	15.53	L3(C1-C2)	59.29
	C3	20.12	L5(C3-C5)	452.76
	C4	18.41	L4(C4-C6)	380.44

Sample	Pore identification code	Pore radius (µm)	Distance identification code (Ci-Ci+n)	Distance (µm)
	C5	8.52	-	-
	C6	16.86	-	-
	C7	10.16	-	-
M II	C1	7.07		
	C2	4.83	L1(C1-C2)	187.98
	C3	3.96	L2(C3-C4)	37.07
	C4	3.58		

An EDX was performed to complete the microstructure analysis. The sections shown in Fig. 3 were selected for this analysis. The results are shown in Fig. 4 and Table 7.

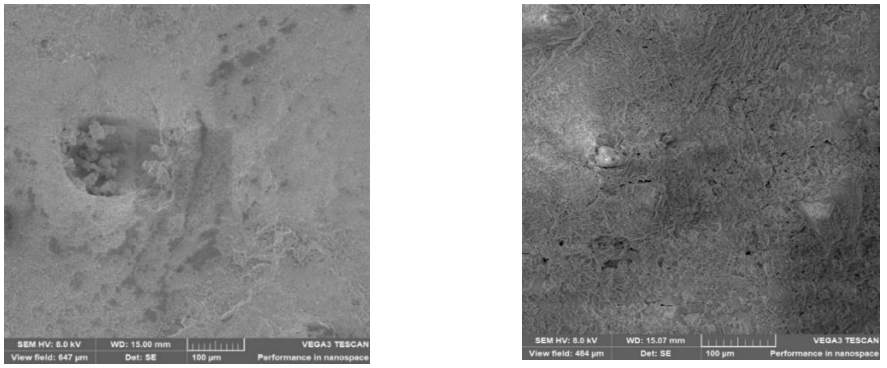

a) b)

Fig. 3. Images on which the elemental analysis of the mortar microstructure was performed: a) MI-100% cement; b) MII -50% GGBS

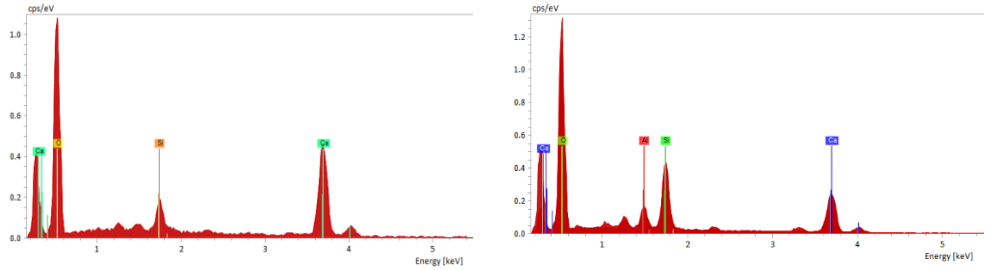

a) b)

Fig. 4. EDX spectrum of: a) MI-100% cement; b) MII -50% GGBS mortar samples

Table 7. Element concentrations (%) in M I, M II obtained by mapping the sample surface at 7 days.

Mortar	O	Ca	Si	Al	Ca/Si
M I	48.47	47.33	4.21	-	11.24
M II	53.13	30.40	13.77	2.70	2.21

In the two samples analyzed, the predominant element, along with oxygen, is calcium, followed by silicon. In addition, Al compounds were observed in the MII sample, probably due to the presence of higher amounts of Al_2O_3 in GGBS, Ref. [40].
The different variations of the Ca/Si ratio:
- for M I with 100% cement, the value of 11.24 indicates the presence of the majority of the calcium-based structure.

- for M II with 50%GGBS the value of 2.21 belongs to the interval (1.2÷2.3) indicating the presence of different forms of C-S-H in the slag sample [41], [42].

The results of the EDX analysis confirm and complement the examination of the SEM images. EDX analysis suggests the presence of C-S-H in MII, which is the main hydration product of cement with a non-crystalline structure [43] and contains a large number of pores that can result in a more porous surface compared to MI.

Characterization of physico-mechanical properties of ACBFS slag

The oxide composition of the air-cooled ACBFS slag shown in Table 8 and the properties of the ACBFS aggregates in Table 9 were analyzed using EN 12620.

Table 8. *Oxide composition of ACBFS air-cooled blast furnace slag (%)

SiO_2	CaO	Al_2O_3	MgO	FeO	MnO	K_2O	Na_2O	S
39.01	41.37	9.14	7.57	0.58	0.64	0.64	0.01	0.51

Note: (*) Chemical characteristics tested by the manufacturer

In ACBFS slag that has been stored for a long time, the iron oxides react expansively, causing the slag particles to disintegrate [44]. To prevent this process the iron oxide content is limited below the value of 3%, according to IS: 383 [45] and the total sulphate content below 2% according to EN 12620. In concretes exposed to wet/dry cycling, ettringite crystals slowly grow and recrystallize to form secondary ettringite, which affects concrete quality [46] The potential for excessive calcium sulfide (CaS) development must be minimized to eliminate the danger of secondary ettringite formation by limiting the total sulfur content below 2% and the acid-soluble sulfate content to a maximum of 0.5%, in accordance with ASTM C114, Section 6 [47]. It is observed in Table 8 and 9 that the recorded values for iron oxide content of 0.58% and sulfur content <1%, are in agree with IS: 383 [45], except for acid soluble sulphate which is 1% above the recommended value of 0.5%.

Table 9. *Physico-mechanical properties of ACBFS air-cooled blast furnace slag.

Physical and chemical characteristics	Recorded values ACBFS	EN 12620 limits	Observations
* Granulosity	G_F 85	G_F 85	
*Content of fine particles below 0.063 mm -f, (%)	f3	(3 ÷22)	
*Soluble chlorines (%)	0.0026	1.1...1.4	
*Total sulfate, (%)	<1	≤ 2.0	< 2.0 ASTM C114
*Acid soluble sulfate content, (16/31.5) mm	AS_1	≤ 1.0	≤ 0.5, ASTM C114
*Content of FeO	0.58		< 3.0 IS:383
*Iron decay	It does not crack or disintegrate	-	
* Decay of silicate calcium	Uniform violet color with evenly distributed light spots in small amounts	-	

Note: (*) Physico-mechanical properties tested by the manufacturer

This deficiency can be overcome by using ACBFS aggregates up to a maximum of 50% as a substitute for natural sand in the composition of road concrete, similar to the recommendations in the guide [48]where the range of 20÷60% for the substitution of natural sand with ACBFS is proposed.

The ACBFS aggregate has a lower actual bulk density (ρ_{rd}), while the fineness modulus or water absorption of WA24 is higher than that of NA sand, values are found in Table 10. The increased absorption indicates the presence of porosity in the ACBFS aggregate and the reduced workability of the fineness modulus (M_f) compared to river sand. The two properties lead to an

increase in the water requirement of the concrete with the given workability [36]. The 24-hour water absorption capacity of ACBFS aggregates is 10% higher than that of sand, which can lead to rapid stiffening, cement hydration retardation and shrinkage cracks in concrete. In order to prevent these undesired effects during concrete production, ACBFS aggregates were used in the state with the SSD dry-saturated surface as well as superplasticizers and air-entraining additives [48].

Table 10. Analysis of physical characteristics of aggregates ACBFS and natural sand NA.

Aggregates	M_f	WA_{24} (SSD)	Absorption capacity at 24 hours	ρ_{rd}
100% (NA)	2.88	2.02%	16.58%	2.55
100%(ACBFS)	2.99	2.56%	26.58%	2.31

The results regarding the susceptibility of ACBFS aggregates to the alkaline silica reaction (ASR) are presented in Fig. 5a) and plotted in the diagram of reduction in sodium hydroxide concentration (Rc) as a function of dissolved silicon dioxide (Sc), Fig. 5b) [49]. The values obtained are consistent with samples tested in Zone A, zone where the aggregates are considered non-reactive according to SR 5440 [31].

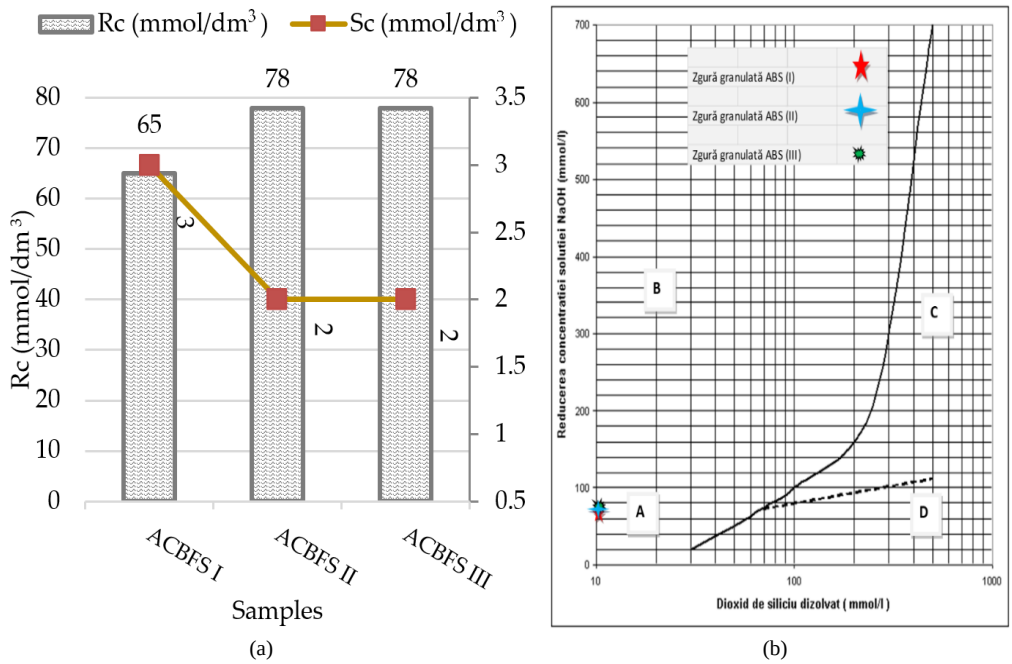

(a) (b)

Fig. 5. (a) Values of sodium hydroxide (Rc) and dissolved silicon dioxide (Sc), in mmol/dm^3; (b) Diagram (Rc -Sc) of the classification of ACBFS aggregates according to the four areas: A, B, C, D

Road concrete mixes with GGBS and ACBFS slag

The recorded results for fresh concrete behavior and at 7-day compressive strengths, Fig. 6, were analyzed to identify the optimal slag-added pavement mix formulation for improved workability, reduced water/binder ratio and compressive strength close to the reference concrete.

In Fig. 6.a) it can be seen that all the samples reached a degree of compaction above the set limit of 1.15%, but with increasing the percentage of river sand substitution by ACBFS, it decreases in the samples of the SI and SII series. The reason for this is that the angular shape and surface roughness of the ACBFS aggregates increase the internal friction between the concrete materials, which in turn affects the decrease in workability [4]. Reducing the cement dosage from

390 to 370 kg/m^3, additive dosages and increasing the w/l ratio of the S II series compared to the S I series resulted in an increase in the degree of compaction, but the compressive strengths were lower, Fig. 6c).

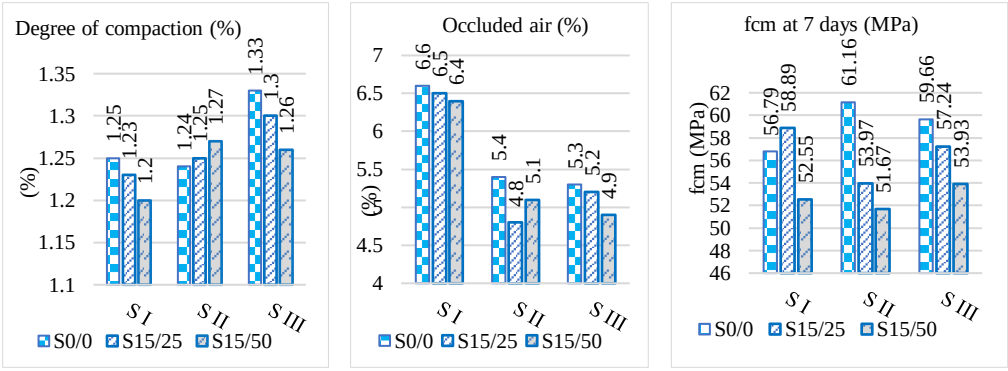

Fig. 6. Road concrete mixtures properties: a) degree of compaction; b) occluded air content; c) average compressive strength at 7 days

Trapped air levels were found to be above 6% for Series I samples and close to 5% for Series SII and SIII samples, Fig. 6b). It is observed that all the strengths obtained are above the minimum value of 50 MPa set for 28 days of age. The highest compressive strengths at 7 days were recorded for the Series III samples. Increasing the w/l ratio resulted in a decrease in compressive strength, with the relationship between the two characteristics being inversely proportional, Fig. 7 a), b), c).

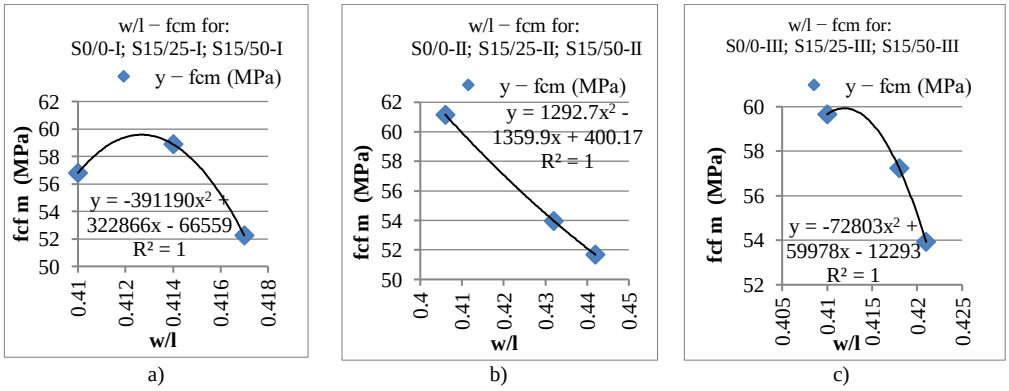

Fig. 7. Relationship between w/l ratio and mean compressive strength fcm

Conclusions

The work was carried out following an experimental test in the laboratory on the possibilities of replacing cement and natural sand with the two types/forms of granulated slag: GGBS (cement) and ACBFS (natural sand). Three series of recipes where cement was replaced by 15% GGBS and sand by 25% and 50% ACBFS were analyzed to select the optimal recipes to meet the specific requirements of fresh and hardened pavement concrete.

The oxidic composition of GGBS type slag indicates a hydraulic and pozzolanic activity when used as a binder in the composition of road concrete. The 7-day activity index determined on mortar samples shows a value that is above the recommended value, at least 45%.

The study of the surface morphology of 100% cement mortar and 50% GGBS mortar aged 7 days shows that the replacement of cement with 50% GGBS favors the formation of the C-S-H hydration product, resulting in a more porous structure for 50% GGBS mortar, then the compact structure in 100% cement mortar.

The content of CaO-free and C_3A in the GGBS slag determined by analytical formulas indicates the possibility of replaying the cement by max. 22%, so that they are within the permissible limits of the reference standard.

The chemical analysis of the ACBFS type slag aggregates shows that they do not react with alkaline silica and that they have an adequate content of chemical elements, which recommends them as substitutes for natural sand in a maximum percentage of 50%.

Higher proportions of ACBFS-type slag as a substitute for sand lead to an increase in the content of acid-soluble sulfate beyond the allowable limit and an increase in the water-cement ratio to achieve workability, since the fineness modulus and water absorption coefficient are higher than that of natural sand.

Regarding the performance of the pavement composites evaluated at 7 days, Series III is selected to continue the experimental programs as it shows the best results: increased workability, reduced water/cement ratio and high compressive strengths and low cement content.

The physicochemical properties of GGBS slag as a substitute for cement and ACBFS aggregates as a substitute for natural sand (0/4) mm encourage their widespread use in the composition of road concrete.

However, the proportions of cement and natural sand that are substituted by blast furnace slag (GGBS and ACBFS) are determined when designing the mixtures in such a way that the percentage content of the chemical components in the slag used complies with the limited permissible values.

Acknowledgments

This paper was financially supported by the Project “Network of excellence in applied research and innovation for doctoral and postdoctoral programs/InoHubDoc”, project co-funded by the European Social Fund financing agreement no. POCU/993/6/13/153437. (D.S.) acknowledge the financial support by the Ministry of Research, Innovation, and Digitization through Program 1—Development of the national research & development system, Subprogram 1.2—Institutional performance—Projects that finance the RDI excellence, Contract no.18PFE / 30.12.2021.

References

[1] P. Hajek, *Concrete Structures for Sustainability in a Changing World*, **Procedia Eng.**, **171**, 2017, pp. 207–214.

[2] K. P. Mehta, *Reducing the environmental impact of concrete*, ***Concr. Int***, **23(10)**, 2001, pp. 61–66.

[3] O. Corbu, D. V Bompa, and H. Szilagyi, *Eco-efficient cementitious composites with large amounts of waste glass and plastic*, **Proc. Inst. Civ. Eng. - Eng. Sustain.**, **175(2)**, 2022, pp. 64–74.

[4] J. Ahmad *et al.*, *A Comprehensive Review on the Ground Granulated Blast Furnace Slag (GGBS) in Concrete Production*, **Sustain.,** 14(14), 2022, p. 8783.

[5] R. D. Cadar, R. M. Boitor, and M. L. Dragomir, *An Analysis of Reclaimed Asphalt Pavement*

from a Single Source—Case Study: A Secondary Road in Romania, **Sustain., 14(12)**, 2022, p. 7057.

[6] M. L. Dragomir, R. D. Cadar, and R. M. Boitor, *Using E-waste in asphalt mixtures – a laboratory investigation*, **IOP Conf. Ser. Mater. Sci. Eng.**, **1138(1)**, 2021, p. 012022.

[7] C. Dimulescu and A. Burlacu, *Industrial Waste Materials as Alternative Fillers in Asphalt Mixtures*, **Sustainability**, **13(14)**, 2021, p. 8068.

[8] A. Forton, S. Mangiafico, C. Sauzéat, H. Di Benedetto, and P. Marc, *Behaviour of binder blends: experimental results and modelling from LVE properties of pure binder, RAP binder and rejuvenator*, **Road Mater. Pavement Des.**, **22(1)**, 2021, pp. S197–S213.

[9] A. Forton, S. Mangiafico, C. Sauzéat, H. Di Benedetto, and P. Marc, *Properties of blends of fresh and RAP binders with rejuvenator: Experimental and estimated results*, **Constr. Build. Mater.**, **236**, 2020, p. 117555.

[10] M. L. Dragomir, A. F. Clitan, and N. Pop, *Using the Waste of Polyester and Glass Fiber in Cold Recycling Highways Superstructure*, in **Advanced Engineering Forum**, **21**, 2017, pp. 309–316.

[11] A. Burlacu and C. Racanel, *Reducing cost of infrastructure works using new technologies*, **3rd International Conference on Road and Rail Infrastructure,Croația,** 2014. https://www.oecd-ilibrary.org/development/road-and-rail-infrastructure-in-asia_9789264302563-en (accessed Feb. 27, 2023).

[12] K. G. Santhosh, S. M. Subhani, and A. Bahurudeen, *Cleaner production of concrete by using industrial by-products as fine aggregate: A sustainable solution to excessive river sand mining*, **J. Build. Eng.**, **42**, 2021, p. 102415.

[13] K. P. Verian, P. Panchmatia, J. Olek, and T. Nantung, *Pavement concrete with air-cooled blast furnace slag and dolomite as coarse aggregates*: *Effects of deicers and freeze-thaw cycles*, **Transp. Res. Rec.**, **2508(1)**, 2015, pp. 55–64.

[14] L. Koehnken and M. Rintoul, *Impacts of sand mining on ecosystem structure*, **Process Biodivers. Rivers**,2018 WWF, Switz.

[15] A. Lăzărescu, B. A. Ionescu, and A. Hegyi, *Alkali-activated fly ash-based geopolymer concrete containing spent garnet as replacement for sand*, **EJMSE**, **8(1)**, 2023, pp. 11–21.

[16] Y.-H. Feng *et al.*, *Research status of centrifugal granulation, physical heat recovery and resource utilization of blast furnace slags*, **J. Anal. Appl. Pyrolysis**, **157**, 2021, p. 105220.

[17] Article, **Viatalibera.ro**, 2022. https://www.g4media.ro/combinatul-siderurgic-din-galati-a-inregistrat-in-2021-cea-mai-mare-productie-de-otel-din-ultimii-12-ani.html (accessed Apr. 29, 2023).

[18] T. Ozbakkaloglu, L. Gu, and A. Fallah Pour, *Normal- and high-strength concretes incorporating air-cooled blast furnace slag coarse aggregates: Effect of slag size and content on the behavior*, **Constr. Build. Mater.**, **126**, 2016, pp. 138–146.

[19] S. Prakash, S. Kumar, R. Biswas, and B. Rai, *Influence of silica fume and ground granulated blast furnace slag on the engineering properties of ultra-high-performance concrete*, **Innov. Infrastruct. Solut.**, **7(1)**, 2021, p. 117.

[20] J. Ahmad *et al.*, *Effects of steel fibers (Sf) and ground granulated blast furnace slag (ggbs) on recycled aggregate concrete*, **Materials (Basel).**, **14(24)**, 2021, p. 7497.

[21] H. K. Hamzah, D. P. Georgescu, N. H. A. Khalid, and G. F. Hussein, *Strength performance of free cement mortars incorporating fly ash and slag: effects of alkaline activator solution dosage*, **Open J. Sci. Technol.**, **3(2)**, 2020, pp. 87–98.

[22] R. K. Patra and B. B. Mukharjee, *Influence of incorporation of granulated blast furnace slag as replacement of fine aggregate on properties of concrete*, **J. Clean. Prod.**, **165**, 2017,

pp. 468–476.
[23] W. Aiguo, L. Peng, L. Kaiwei, L. Yan, Z. Gaozhan, and S. Daosheng, *Application of Air-cooled Blast Furnace Slag Aggregates as Replacement of Natural Aggregates in Cement-based Materials*: *A Study on Water Absorption Property*, **J. Wuhan Univ. Technol. Sci. Ed**.2018 *www.jwutms.net Apr.2018 445.*
[24] R. Kumar, S. Sen, and R. V Ramna, *Utilization of air-cooled blast furnace slag as a 100% replacement of river sand in mortar and concrete*, **Indian Concr. J**., **96(7)**, 2022, pp. 6-21.
[25] J. Shi, J. Tan, B. Liu, J. Chen, J. Dai, and Z. He, *Experimental study on full-volume slag alkali-activated mortars: Air-cooled blast furnace slag versus machine-made sand as fine aggregates*, **J. Hazard. Mater.**, 403, 2021, p. 123983.
[26] S. Saluja, S. Goyal, and B. Bhattacharjee, *Strength properties of roller compacted concrete containing GGBS as partial replacement of cement*, **J. Eng. Res**.2019, vol. 7, no. 1.
[27] I. M. Nicula L.M., Corbu O., *The effect of recycled blast furnace slag waste on the characteristics and durability of cement-based mortars*, **Int. Multidiscip. Sci. GeoConference Surv. Geol. Min. Ecol. Manag. SGEM 18(6.3),** 2018, *pp. 379-390.*
[28] *SR 667 Natural aggregates and processed stone for roads*. **ASRO Bucharest**, 2001.
[29] *NE 014:2002 The norm for the execution of cement concrete road pavements in a fixed and sliding formwork system*. **Matrix ROM, Bucharest**, 2007, ISBN 978-973-755-185-6.
[30] A. Moanță, *Use the ESP dust as admixture and additional constituent in cement grinding*, **Build. Mater**.2004, vol. XXXIV, nr.1.
[31] *SR 5440 Tests on cement concrete. Checking the alkali-aggregate reaction.* **ASRO Bucharest,** 2009.
[32] *SR 648 Granulated blast furnace slag for the cement industry*. **ASRO Bucharest,** 2002.
[33] *Metallurgical slags and thermal power plant ashes*. **https:**//www.creeaza.com/tehnologie/tehnica-mecanica/ZGURILE-METALURGICE-SI-CENUSIL756.php (accessed Sep. 05, 2023).
[34] B. Lothenbach, K. Scrivener, and R. D. Hooton, S*upplementary cementitious materials*, **Cem. Concr. Res**., **41(12)**, 2011, pp. 1244–1256.
[35] *D6868 Standard; Specification for Biodegradable Plastics Used as Coatings on Paper and Other Compostable Substrates*, **ASTM Int. West Conshohocken, PA, USA,** 2017.
[36] I.Ionescu;T.Ispas, *The properties and technology of concrete*, in **Bucharest technical publishing house**, 1997.
[37] A. F. Simedru, A. Becze, O. Cadar, D. A. Scurtu, D. Simedru, and I. Ardelean, Structural *Characterization of Several Cement-Based Materials Containing Chemical Additives with Potential Application in Additive Manufacturing*, **Int. J. Mol. Sci**., **24(9)**, 2023, p. 7688.
[38] L. M. Nicula, O. Corbu, I. Ardelean, A. V Sandu, M. Iliescu, and D. Simedru, Freeze–*Thaw Effect on Road Concrete Containing Blast Furnace Slag: NMR Relaxometry Investigations*, **Mater. -ISSN 1996-1944, Mater.**, **14(12)**, 2021, p. 3288.
[39] ACI-233R-03, *Slag Cement in Concrete and Mortar*,2003, **American Concrete Institute**.
[40] J. Lee and S. Choi, *Case Studies in Construction Materials Effect of replacement ratio of ferronickel slag aggregate on characteristics of cementitious mortars at different curing temperatures*, **Case Stud. Constr. Mater**., **18(9)**, 2023, p. e01882.
[41] I. G. Richardson, *The nature of C-S-H in hardened cements*, **Cem. Concr. Res**., **29(8)**, 1999, pp. 1131–1147.
[42] D. C. Chu, J. Kleib, M. Amar, M. Benzerzour, and N.-E. Abriak, *Determination of the degree of hydration of Portland cement using three different approaches: Scanning electron microscopy (SEM-BSE) and Thermogravimetric analysis (TGA)*, **Case Stud. Constr.**

Mater., **15**, 2021, p. e00754,
[43] *Calcium Silicate Hydrate*, https://www.sciencedirect.com/science/article/pii/B9780081006931000084.
[44] L. M. Juckes, *Dicalcium Silicate in Blast-Furnace Slag: A Critical Review of the Implications for Aggregate Stability*, **Miner. Process. Extr. Metall., 111(3)**, 2002, pp. 120–128(9).
[45] *IS: 383 (2016). 'Coarse and fine aggregate for concrete – specification', Bureau of Indian Standards, New Delhi, India*. https://archive.org/details/gov.in.is.383.2016/page/n5/mode/2up (accessed Apr. 22, 2023).
[46] W. Kurdowski, *Cement and Concrete Chemistry*. **Springer Netherlands**, 2014.
[47] K. D. Smith, D. A. Morian, and T. J. Van Dam, *Use of Air-Cooled Blast Furnace Slag as Coarse Aggregate in Concrete Pavements—A Guide to Best Practice*. **Report No. FHWA-HIF-12-009**, 2012.
[48] ACI 213R-03, *Guide for Structural Lightweight Aggregate Concrete*, **Am. Concr. Inst. Farmingt. Hills, MI.,** 2003.
[49] N. Liliana Maria, "Thesis: Research and studies on the durability of blast furnace slag road concretes, BcR-S.," Cluj-Napoca Technical University, 2021.

Received: May 01, 2023
Accepted: June 09, 2023